Inorganic−Organic Hybrid Compounds: Synthesis, Structure, and Magnetic Properties of the First Organically Templated Iron Oxalate−Phosphite, $[C_4N_2H_{12}][Fe^{II}_4(HPO_3)_2(C_2O_4)_3]$, Possessing Infinite Fe−O−Fe Chains

Sukhendu Mandal,[†] Swapan K. Pati,[‡] Mark A. Green,[§] and Srinivasan Natarajan*,[†]

Framework Solids Laboratory, Solid State and Structural Chemistry Unit, Indian Institute of Science, Bangalore 560 012, India, Theoretical Sciences Unit, Jawaharlal Nehru Centre for Advanced Scientific Research, Jakkur P.O., Bangalore 560 064, India, and Davy-Faraday Research Laboratory, The Royal Institution of Great Britain, 21 Albemarle Street, London W1S 4BS, United Kingdom

Received January 28, 2005. Revised Manuscript Received March 23, 2005

A hydrothermal reaction of a mixture containing iron(II) oxalate dihydrate, phosphorus acid, piperazine, and water at 150 °C for 72 h gave light-yellow cubes of a new hybrid iron oxalate−phosphite, $[C_4N_2H_{12}][Fe^{II}_4(HPO_3)_2(C_2O_4)_3]$, **I**. The structure, formed by FeO_6, HPO_3, and oxalate building units, possesses infinite one-dimensional chains of Fe−O−Fe, formed by Fe_2O_{10} dimers. The phosphite units are grafted to these chains, and the oxalate moieties bond with the iron center through *in-plane* and *out-of-plane* connectivity forming a three-dimensional structure with intersecting channels. The organic amine molecule occupies the middle of the channels. The connectivity between the phosphite units and the Fe−O−Fe chains resembles the tancoite structure. Magnetic investigations reveal that the iron is present in the +2 oxidation state and orders antiferromagnetically.

Introduction

Intense research activity in the area of open-framework metal phosphates during the last two decades gave rise to a large number of new compounds with novel structures of varying dimensionality.[1] Of these, iron phosphates occupy an important position.[2−4] Metal−organic framework (MOF) compounds have also been gaining much interest recently for their many interesting structures and properties.[5−7] Recently, the pseudotetrahedral phosphite group was successfully employed as a building unit giving rise to a new series of framework compounds.[8−10] Oxalate anions have also been used in the preparation of inorganic−organic hybrid compounds, resulting in oxalatophosphate frameworks. A large number of oxalatophosphates of transition and main-group elements have been prepared and characterized during the past few years.[11−15] The oxalatophosphates generally adopt three-dimensional framework structures, though lower-dimensional structures have also been prepared. The oxalatophosphite frameworks, on the other hand, have not been explored hitherto. We have been interested to investigate the formation of new bifunctional inorganic−organic hybrid frameworks incorporating the phosphite ligand.[16] To this end, we have now prepared an organically templated oxalatophosphite, $[C_4N_2H_{12}][Fe^{II}_4(HPO_3)_2(C_2O_4)_3]$, **I**, with three-dimensional structure. In addition to being the first oxalatophosphite hybrid compound, **I** is original in that it possesses a unique one-dimensional Fe−O−Fe chains. The compound orders antiferromagnetically at low temperatures. In this paper, we present the synthesis, structure, and magnetic properties of this compound.

Experimental Section

Synthesis and Initial Characterization. The iron oxalatophosphite, $[C_4N_2H_{12}][Fe^{II}_4(HPO_3)_2(C_2O_4)_3]$, **I**, was synthesized under

* Corresponding author. E-mail: snatarajan@sscu.iisc.ernet.in.
† Indian Institute of Science.
‡ Jawaharlal Nehru Centre for Advanced Scientific Research.
§ The Royal Institution of Great Britain.

(1) Cheetham, A. K.; Loiseau, T.; Ferey, G. *Angew. Chem., Int. Ed*. **1999**, *38*, 3268.
(2) Moore, P. B. *Crystallochemical Aspects of the Phosphate Minerals*; Niagru, J. O., Moore, P. B., Eds.; Springer-Verlag: Berlin, 1984; p 155.
(3) Riou-Cavellec, M.; Riou, D.; Ferey, G. *Inorg. Chem. Acta* **1999**, *291*, 317.
(4) Lii, K.-H.; Hyang, R.-F.; Zima, V.; Huang, C.-Y.; Lin, H.-M.; Jiang, J.-C.; Liao, F.-L.; Wang, S.-L. *Chem. Mater*. **1998**, *10*, 2599.
(5) Rao, C. N. R.; Natarajan, S.; Vaidhyanathan, R. *Angew. Chem., Int. Ed*. **2004**, *43*, 1466.
(6) Eddaoudi, M.; Kim, J.; Vodak, D.; Sudik, A.; Wachter, J.; O'Keeffe, M.; Yaghi, O. M. *Proc. Nat. Acad. Sci., U.S.A.* **2002**, *99*, 4900.
(7) Ockwig, N. W.; Delgado-Friedrichs, O.; O'Keeffe, M.; Yaghi, O. M. *Acc. Chem. Res*. **2005**, DOI 10.1021/ar200221 and the references therein.
(8) Harrison, W. T. A.; Philips, M. L. F.; Stranchfield, J.; Nenoff, T. M. *Inorg. Chem*. **2001**, *40*, 895.
(9) Fernandez, S.; Mesa, J. L.; Pizarro, J. L.; Lezama, L.; Arriortua, M. I.; Rojo, T. *Angew. Chem., Int. Ed.* **2002**, *41*, 3683.
(10) Fu, W. S.; Wang, L.; Shi, Z.; Li, G. H.; Chen, X. B.; Dai, Z. M.; Yang, L.; Feng, S. H. *Cryst. Growth Des.* **2004**, *4*, 297.
(11) Lin, H. M.; Lii, K. H.; Jiang, Y. C.; Wang, S. L. *Chem. Mater*. **1999**, *11*, 519.
(12) Lethbridge, Z. A. D.; Hiller, A. D.; Cywinske, R.; Lightfoot, P. *J. Chem. Soc., Dalton Trans*. **2000**, 1595.
(13) Choudhury, A.; Natarajan, S.; Rao, C. N. R. *Chem.−Eur. J*. **2000**, *6*, 1168.
(14) Do, J.; Bontchev, R. P.; Jacobson, J. *Chem. Mater*. **2001**, *13*, 2601.
(15) Jiang, Y. C.; Wang, S. L.; Lii, K. H.; Nguyen, N.; Ducouret, A. *Chem. Mater*. **2003**, *15*, 1633.
(16) Mandal, S.; Pati, S.; Green, M. A.; Natarajan, S. *Chem. Mater.*, in press.

10.1021/cm0501968 CCC: $30.25
Published on Web 04/30/2005

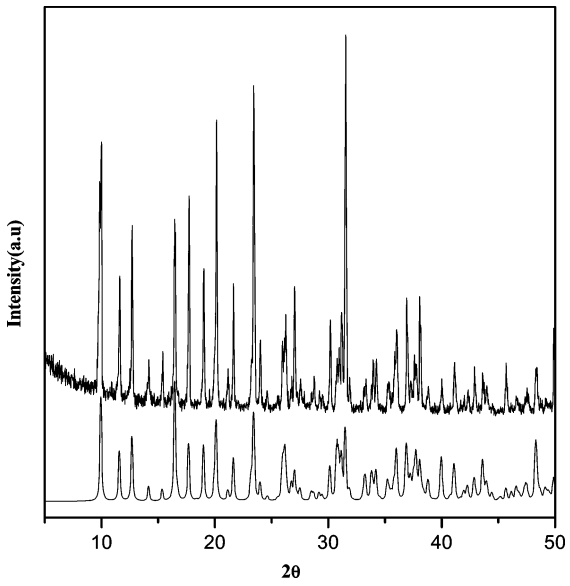

Figure 1. Powder XRD pattern (Cu Kα) of $[C_4N_2H_{12}][Fe^{II}_4(HPO_3)_2(C_2O_4)_3]$, **I**. (a) (a) Experimental; (b) simulated.

hydrothermal conditions using iron(II) oxalate dihydrate as the source of iron. In a typical synthesis, 0.279 g of iron(II) oxalate dihydrate was dissolved in 7 mL of deionized water. To this, 0.318 g of H_3PO_3 was added. Finally, 0.334 g of piperazine (PIP) was added to the mixture and homogenized for 30 min at room temperature. The final mixture with the composition, 1.0 $FeC_2O_4 \cdot 2H_2O$:2.0 H_3PO_3:2.0 (PIP):200 H_2O, was transferred in to a 23-mL acid-digestion bomb and heated at 150 °C for 72 h. The resulting product contained only light-yellow-color cubelike single crystals in large quantities. The crystals were filtered, washed with deionized water, and dried at ambient conditions. The yield of the product was ∼80% based on Fe. The initial and final pH of the reaction mixture was ∼4.

The initial characterization was carried out using powder X-ray diffraction (XRD), thermogravimetric analysis (TGA), and infrared (IR) measurements. An EDAX analysis on many single crystals indicated an Fe:P ratio of 2:1, consistent with the single-crystal X-ray data. The powder XRD patterns were recorded on crushed single crystals in the 2θ range 5−50° using Cu Kα radiation (Philips X'pert). The XRD pattern was entirely consistent with the structure determined using the single-crystal XRD. The observed and simulated XRD pattern is shown in Figure 1.

TGA has been carried out (Mettler-Toledo, TG850) in oxygen atmosphere (flow rate = 50 mL/min) in the temperature range 25−800 °C (heating rate = 5 °C/min^{-1}). The studies show a single sharp weight loss in the range 375−450 °C. The total observed weight loss was found to be 37.45%. In most of the framework compounds, this weight loss, under the flow of oxygen, generally corresponds to the loss of the organic amine and the decomposition of the oxalate units. The final decomposed products of **I** identified by powder XRD were $Fe^{III}P^{V}O_4$ (JCPDS 17-0837) and $Fe_2^{III}O_3$ (JCPDS 47-1409). The calculated weight loss due to decomposition of organic amine and oxalate moiety is 47.88%, but the observed weight loss was only 37.45%. This discrepancy between the calculated and observed weight loss in the TGA studies of **I** can be explained by considering the oxidation of Fe^{II} to Fe^{III} and P^{III} to P^{V} during the decomposition. In oxygen atmosphere, the anionic framework of **I** was oxidized to a mixture of $Fe_2^{III}O_3$ and $Fe^{III}P^{V}O_4$ powders, and the remaining products were gases (CO_2 and H_2O). From the molecular formula, the calculated gain in weight due to the oxidation of Fe^{II} to Fe^{III} and P^{III} to P^{V} were 6.52 and 4.35%, respectively. Thus, during the TGA studies, the competition between the weight loss due to the decomposition of the occluded amine and the oxalate units and the weight gain due to the oxidation of the Fe^{II} and P^{III} ions resulted in a net lower observed weight loss. The diprotonated organic amine molecule, during the decomposition, contributed two protons. By consideration of this to be the equilibrium, the net weight loss will be 37.45 + 6.52 + 4.35 = 48.32%, which matches very well with the expected calculated total weight loss (47.88%). The decomposition of **I** can be understood as follows

$$[Fe_4^{II}(C_2O_4)_3(HP^{III}O_3)_2]^{2-} + 2(H^+) + 3.5(O_2) \rightarrow Fe_2^{III}O_3 + 2Fe^{III}P^{V}O_4 + 6CO_2(g)\uparrow + 2H_2O(g)$$

IR spectroscopic studies carried out in the range 400−4000 cm^{-1} using the KBr pellet method (Bruker IFS-66v) exhibited typical peaks corresponding to the piperazine, oxalate, and HPO_3 moieties. IR bands: ν(NH) = 3015 cm^{-1}, ν(CH) = 2970 cm^{-1}, ν(PH) = 2390 cm^{-1}, ν_{as}(CO) = 1655 cm^{-1}, δ(NH) = 1605 cm^{-1}, δ(CH) = 1480 cm^{-1}, ν_s(CO) = 1420 cm^{-1}, $\nu_{as}(PO_3)$ = 1137 cm^{-1}, δ(HP) = 1045 cm^{-1}, $\nu_s(PO_3)$ = 1006 cm^{-1}, $\delta_s(PO_3)$ = 600 cm^{-1}, $\delta_{as}(PO_3)$ = 492 cm^{-1}.

The temperature variation of the magnetic susceptibility studies has been carried out on powdered single crystals in the range 3−300 K with a SQUID magnetometer (Quantum Design Inc., USA).

Single-Crystal Structure Determination. A suitable colorless single crystal was carefully selected under a polarizing microscope and glued to a thin glass fiber with cyanoacrylate (superglue) adhesive. Crystal structure determination by XRD was performed on Siemens SMART-CCD diffractometer equipped with a normal focus and a 2.4-kW sealed-tube X-ray source (Mo Kα radiation, λ = 0.71073Å) operating at 40 kV and 40 mA. A hemisphere of intensity data was collected at room temperature in 1321 frames with ω scans (width of 0.30° and exposure time of 10 s per frame) in the 2θ range 3−46.5°. Pertinent experimental details for the structure determination of **I** are presented in Table 1.

Table 1. Crystal Data and Structure Refinement Parameters for $[C_4N_2H_{12}][Fe_4^{II}(C_2O_4)_3(HPO_3)_2]$, I[a]

empirical formula	$Fe_2P_1O_9C_5N_1H_7$
formula weight	367.7723
crystal system	monoclinic
space group	$P2_1/c$ (no.14)
a (Å)	7.7286(2)
b (Å)	7.5874(2)
c (Å)	17.9816(3)
β (deg)	98.2140(10)
volume (Å^3)	1043.62(4)
Z	4
T (K)	293(2)
ρ_{calc} (g cm^{-3})	2.341
μ (mm^{-1})	2.976
θ range (deg)	2.29−23.28
λ (Mo Kα) (Å)	0.71073
total data collected	4263
unique data	1503
refinement method	full-matrix least-squares on $\|F^2\|$
R_{merg}	0.0278
R indexes [$I > 2\sigma(I)$]	$R_1 = 0.0298$, w$R_2 = 0.0790$
R (all data)	$R_1 = 0.0330$, w$R_2 = 0.0811$
goodness of fit (S_{obs})	1.082
no. variables	164
largest difference map hole and peak e Å^{-3}	1.237 and −0.549

[a] $R_1 = \sum||F_o| - |F_c||/\sum|F_o|$; w$R_2 = \{\sum[w(F_o^2 - F_c^2)]/\sum[w(F_o^2)^2]\}^{1/2}$. $w = 1/[\rho^2(F_o)^2 + (aP)^2 + bP]$. P = [max($F_o$, O) + 2($F_c$)^2]/3, where $a = 0.0345$ and $b = 4.0050$.

Table 2. Selected Bond Distances and Angles in $[C_4N_2H_{12}][Fe_4^{II}(C_2O_4)_3(HPO_3)_2]$, I[a]

bond	distance, Å	bond	distance, Å
Fe(1)−O(1)	2.000(3)	Fe(2)−O(4)	2.130(3)
Fe(1)−O(2)	2.077(3)	Fe(2)−O(9)	2.135(3)
Fe(1)−O(3)	2.102(3)	Fe(2)−O(3)	2.223(3)
Fe(1)−O(4)	2.122(3)	Fe(2)−O(6) #1	2.397(3)
Fe(1)−O(5)	2.217(3)	P(1)−O(7) #2	1.504(3)
Fe(1)−O(6)	2.277(3)	P(1)−O(1) #1	1.525(3)
Fe(2)−(7)	1.981(3)	P(1)−O(4)	1.529(3)
Fe (2)−O (8)	2.124(3)		

angle	amplitude (deg)	angle	amplitude (deg)
O(1)−Fe(1)−O(2)	152.11(12)	O(1)−Fe(1)−O(3)	101.01(12)
O(2)−Fe(1)−O(3)	101.13(12)	O(1)−Fe(1)−O(4)	107.97(12)
O(2)−Fe(1)−O(4)	92.56(12)	O(3)−Fe(1)−O(4)	79.57(11)
O(1)−Fe(1)−O(5)	84.96(12)	O(2)−Fe(1)−O(5)	83.70(12)
O(3)−Fe(1)−O(5)	77.04(11)	O(4)−Fe(1)−O(5)	155.09(11)
O(1)−Fe(1)−O(6)	84.17(11)	O(2)−Fe(1)−O(6)	76.55(11)
O(3)−Fe(1)−O(6)	170.39(11)	O(4)−Fe(1)−O(6)	91.16(11)
O(5)−Fe(1)−O(6)	111.69(11)	O(7)−Fe(2)−O(8)	170.02(12)
O(7)−Fe(2)−O(4)	100.26(13)	O(8)−Fe(2)−O(4)	89.70(11)
O(7)−Fe(2)−O(9)	92.53(12)	O(8)−Fe(2)−O(9)	77.52(11)
O(4)−Fe(2)−O(9)	164.19(12)	O(7)−Fe(2)−O(3)	89.61(12)
O(8)−Fe(2)−O(3)	91.97(12)	O(4)−Fe(2)−O(3)	76.74(11)
O(9)−Fe(2)−O(3)	94.23(11)	O(7)−Fe(2)−O(6) #1	85.98(12)
O(8)−Fe(2)−O(6) #1	92.74(11)	O(4)−Fe(2)−O(6) #1	102.01(10)
O(9)−Fe(2)−O(6)#1	88.03(10)	O(3)−Fe(2)−O(6)#1	175.13(11)
P(1)#2−O(1)−Fe(1)	128.66(18)	P(1)−O(4)−Fe(1)	124.51(17)
P(1)−O(4)−Fe(2)	129.09(17)	Fe(1)−O(4)−Fe(2)	102.48(12)
P(1)#1−O(7)−Fe(2)	135.08(19)	Fe(1)−O(6)−Fe(2)#2	108.52(11)
Fe(1)−O(3)−Fe(2)	100.05(11)	C(4)−O(2)−Fe(1)	117.3(3)
C(5)#4−O(3)−Fe(1)	117.1(3)	C(5)#4−O(3)−Fe(2)	139.5(3)
C(5)−O(5)−Fe(1)	112.2(3)	C(3)#3−O(6)−Fe(1)	108.52(11)
C(3)#3−O(6)−Fe(2)#2	129.7(3)	C(3)−O(8)−Fe(2)	114.9(3)
C(4)−O(9)−Fe(2)	114.2(3)	O(8)−C(3)−O(6)#5	127.5(4)

[a] Symmetry transformation used to generate equivalent atoms: #1 $-x+1, y-1/2, -z+3/2$; #2 $-x+1, y+1/2, -z+3/2$; #3 $x-1, y, z$; #4 $-x+1, -y, -z+1$; #5 $x+1, y, z$.

An empirical absorption correction was applied using the SADABS program.[17] The structure was solved and refined using the SHELXL suit of programs.[18] The direct method solution readily revealed sufficient fragments of the structure (Fe, P, and O) and enabled the remainder of the non-hydrogen atoms to be located from difference Fourier maps and the refinements to proceed to $R < 10\%$. The hydrogen atom in the P−H group and all other hydrogen positions were initially located in the difference Fourier map, and for the final refinement the hydrogen atoms were placed in geometrically ideal positions and refined using the riding mode. The last cycles of refinements included atomic positions, anisotropic thermal parameters for all the non-hydrogen atoms, and isotropic thermal parameters for all the hydrogen atoms. Full-matrix-least-squares structure refinement against $|F|^2$ was carried out using the SHELXL package of programs.[18] Selected bond distances and angles for **I** are presented in Table 2.

Results and Discussion

The asymmetric unit of **I** contains 18 non-hydrogen atoms, of which two iron atoms and a phosphorus atom are crystallographically independent. The iron atoms are connected with six oxygen atom neighbors and have octahedral coordination with average Fe−O bond distances of 2.133 and 2.165 Å, respectively. The O−Fe−O bond angles are in the range 76.55(11) − 170.39(11)°. The iron atoms are connected to a phosphorus atom through Fe−O−P bonds and to oxalate groups through Fe−O−C bonds with average bond angles of 129.3 and 120.1°, respectively. The iron atoms are also connected to each other through three-coordinated oxygen atoms (O(3), O(4), and O(6)) with average Fe−O−Fe bond angles of 103.7°. The P−O distances have an average value of 1.519 Å. All the other bond distances and angles are in the range expected for this type of bonding and matches well with those reported previously in the literature.[11−15]

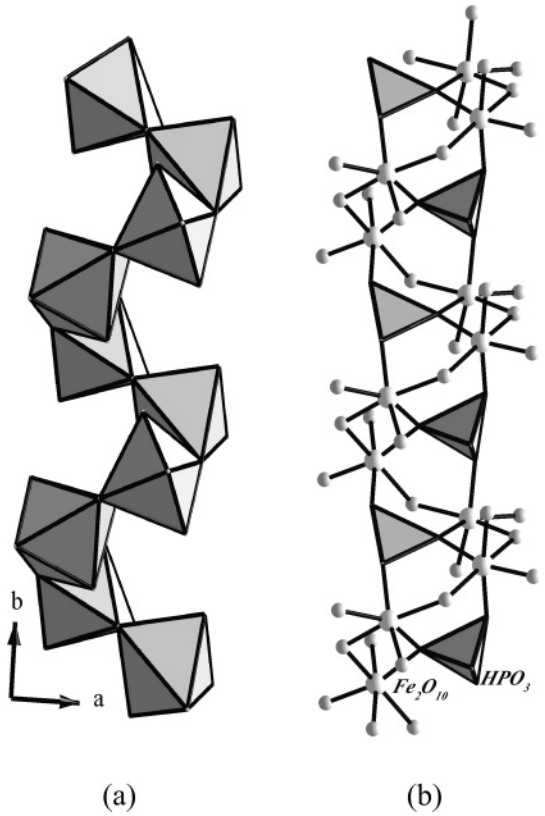

Figure 2. (a) The one-dimensional Fe−O−Fe chain in **I**. (b) The one-dimensional structure formed by the linkage between iron and phosphite units. Oxalate units are not shown for clarity.

The structure of **I** is built up from a linkage involving the FeO_6 octahedra, the HPO_3 pseudotetrahedra, and the oxalate units. The iron atoms are connected to each other through two three-coordinated oxygen atoms (O(3) and O(4)) forming an edge-shared dimer, Fe_2O_{10}. The edge-shared Fe_2O_{10} dimers are arranged around a 2_1 screw axis connected through their corners via another three-coordinate oxygen atom (O(6)), giving rise to infinite one-dimensional chains of Fe−O−Fe (Figure 2a). The pseudotetrahedral phosphite units are grafted on to these chains forming a one-dimensional structure as shown in Figure 2b. The oxalate moieties bond with the iron center through *in-plane* connectivity giving rise to a hybrid layer and by *out-of-plane* connectivity with the hybrid layer forming the three-dimensional structure. This type of connectivity gives rise to two types of channels along the *bc* and *ac* planes as shown in Figures 3 and 4. The diprotonated piperazine molecule occupies the middle of the channels formed by this connectivity and participates in weak hydrogen bond interactions with the framework oxygen atoms.

(17) Sheldrick, G. M. SADABS *Siemens Area Correction Absorption Correction Program*; University of Göttingen: Göttingen, Germany, 1994.
(18) Sheldrick, G. M. *SHELXL-97 Program for Crystal Structure Solution and Refinement*; University of Göttingen: Göttingen, Germany, 1997.

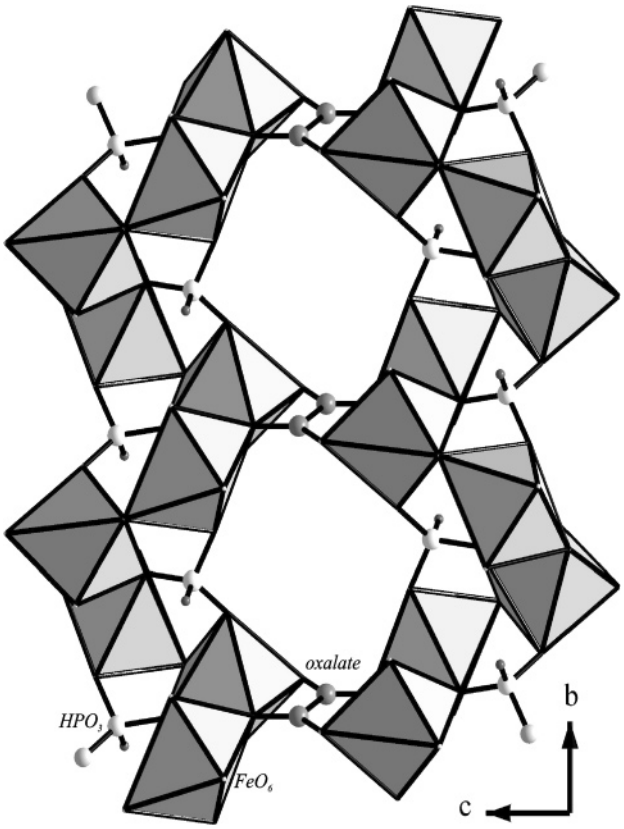

Figure 3. Structure of **I** in the *bc* plane showing the channels. Piperazine molecules occupy these channels (not shown).

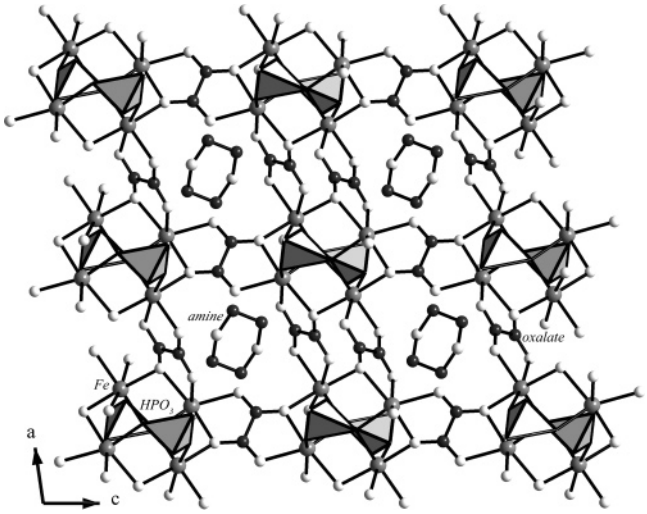

Figure 4. The connectivity between Fe and oxalate units forming an Fe^{II} oxalate three-dimensional structure. The piperazine molecules occupy the channels (see text).

The structure of **I** is closely related to the iron phosphate−oxalate, $[C_4N_2H_{14}][Fe_4(HPO_4)_2(C_2O_4)_3]$, structure reported earlier.[19] **I** has similarities in the connectivity with respect to the iron phosphate−oxalate and the lattice parameters also have comparable values. In the structure of **I**, two FeO_6 octahedra are connected to form the Fe_2O_{10} edge-shared dimers, whereas in the phosphate−oxalate structure FeO_6 and FeO_5 polyhedral units are connected forming the Fe_2O_9 dimers. In **I**, the Fe_2O_{10} dimers are connected through the corners giving rise to an infinite one-dimensional Fe−O−Fe chain. In the phosphate−oxalate structure, on the other hand, the Fe_2O_9 dimers are isolated and are connected by the phosphate groups. Both the compounds have the piperazine molecule in the middle of the channels in the *bc* plane. An alternate description of the structure of **I** could be as a simple Fe^{II} oxalate structure formed by *in-plane* and *out-of-plane* connectivity of the oxalate units, templated by the piperazine molecules. This visualization and description is possible because the phosphite groups do not contribute to the connectivity of the overall structure and appear to decorate only the Fe−O−Fe chains in **I** by linking with three Fe centers through the oxygen atoms (Figure 4). This situation may be contrasted with that of the phosphate−oxalate structure.[19] Fe^{II} oxalate templated by organic amine molecules exhibiting three-dimensional structure has not been described in the literature, though such a structure has been realized in a zinc oxalate containing both the *in-plane* and *out-of-plane* oxalate linkages.[20] It is likely that the combined presence of oxalate and P^{3+} ions might have facilitated the formation of this unusual feature in **I**.

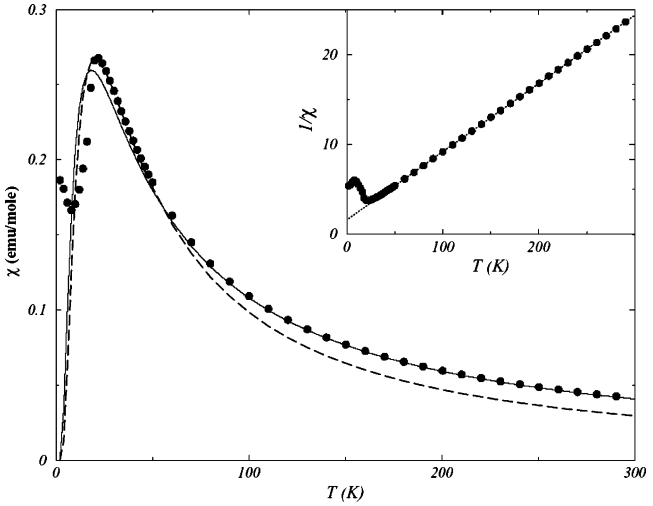

Figure 5. Temperature variation of susceptibility. Inset shows the $1/\chi$ vs T plot. The solid line is a high-temperature fit to the Fisher's formula, and the dashed line is the low-temperature fit (see text).

Magnetic susceptibility studies have been performed in the temperature range 300−4.2 K using a SQUID magnetometer. The studies indicate that the compound orders antiferromagnetically at low temperatures. The temperature variation of the magnetic susceptibility is given in Figure 5. Magnetic investigations show that at very low temperature (~8 K) there is an upward rise in χ as the T is lowered; although above $T = 8$ K, **I** appears to order antiferromagnetically. At high temperatures ($T = 300$ K), the susceptibility value saturates to the paramagnetic spin only value of an Fe^{2+} spin (4.85 μB). A Curie−Weiss fit of the high-temperature data ($T = 100-300$ K) to a form $\chi = (C/T - \theta)$ gives a value of 13.2 and −21.2 K for C and θ, respectively (inset of Figure 5).

Short-range order is generally associated with the low-dimensional antiferromagnetic systems.[21] By assumption of

(19) Choudhury, A.; Natarajan, S.; Rao, C. N. R. *J. Solid State Chem*. **1999**, *146*, 538.

(20) Vaidhyanathan, R.; Natarajan, S.; Cheetham, A. K.; Rao, C. N. R. *Chem. Mater*. **1999**, *11*, 3636.

Chart 1

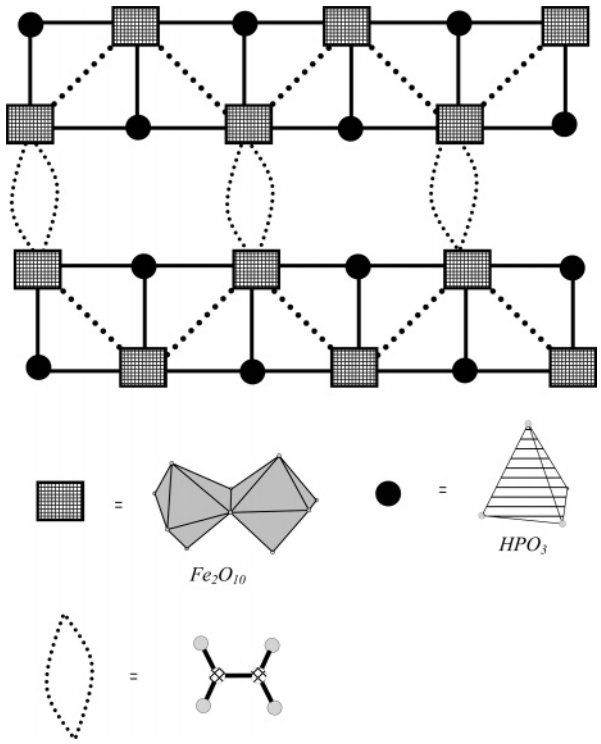

classical spins, Fisher's formula can be used.[22] The high-temperature part can be fitted with an inverse temperature form for χ, equivalent to an expression obtained for dimer, $\chi_{HT} = A \exp(-\Delta/k_BT)/k_BT$. The fitting is shown as a solid line in Figure 5, with $\Delta = 18.4$ K. The low-temperature region ($T \leq 8$ K), however, is not well reproduced by the simple χ_{HT} formula given above. For magnetic excitations corresponding to parabolic magnon dispersion, it has been suggested that a general form of χ can be used: $\chi = A \exp(-\Delta/k_BT)/(k_BT)^{\tau}$, with the exponent τ related to the extended nature of the antiferromagnetic interactions at low temperature.[23] By fitting the above form of the susceptibility with the experimental data, we find that the best fit is obtained with $\Delta = 25.3$ K and $\tau = 1.25$ (dashed line in Figure 5). Clearly this exponent gives the idea of the optimum length scale of the exchange processes in the system at temperatures corresponding to the maximum of χ at $T = \sim 25$ K.

At very low temperature, the susceptibility starts rising as $T \rightarrow 0$, signaling ferromagnetic polarization. It is quite interesting that, in such a small temperature scale, signature of completely opposite exchange processes can be obtained. A careful investigation of the exchange pathways reveals that the dimers of Fe^{2+} are linked by oxygens in the chain direction and through oxalate groups in the other directions (see Chart 1). At high temperature, the dominating exchange processes are through the oxygen atoms, which are clearly antiferromagnetic in nature. This pathway dominates the entire temperature scale down to $T = 8$ K. Below this temperature, however, the system goes through a dimensional crossover, whereby the exchanges between the chains in the planes and in the third direction become dominant. This is because exchanges through the oxalate are very weak and only become relevant at temperatures corresponding to their magnitudes ($J \cong k_BT$). Interestingly, the angle corresponding to the orbital overlap for exchange processes through an oxalate group gives rise to ferromagnetic interactions, although the overlap itself is quite small (not effective). This explains the upward rise of χ below $T = 8$ K. It is quite interesting that the low-temperature thermodynamic properties reveal the three-dimensional couplings, their strength, and characteristic forms. To verify whether there exist any ferromagnetic coupling at low temperature, we have carried out magnetization studies as a function of magnetic field at $T = 2$ K. The low-field magnetization measurements indicate a very small hysteresis loop corresponding to the coupling strength, which is extremely small. The hysteresis loop, however, disappears at very high field.

The alternative explanation for the rise in susceptibility at very low temperature can be through Dzyaloshinsky–Moriya (DM) interactions[24] caused by spin–orbit coupling and differences in the local environments of the adjacent Fe centers. Although DM interactions ($H_{DM} = \Sigma D_{ij} \cdot S_i \times S_j$) are comparatively weaker than the superexchange terms ($H_{SE} = \Sigma J_{ij} \cdot S_i \cdot S_j$) ($D_{ij} \approx J_{ij}/5$], at low temperature, the coupling with other magnetic centers in all three dimensions can give rise to canted magnetic species with weak ferromagnetic polarization.[25] This can, however, be confirmed by changing the groups (with distance as a parameter) in the interchain directions. However, for this system, it is true that either an angle-dependent anti-symmetric exchange or a weak ferromagnetic coupling between the interchain magnetic centers becomes important at very low temperature (<8 K), suggesting a possible change in exchange pathway with dimensional crossover.

From the structural point of view, the structure of **I** presents many unique features. The first and foremost is the presence of infinite one-dimensional Fe–O–Fe chains. Though infinite Fe–O–Fe chains have been observed before in ironphosphates,[26] such a structural feature has not been commonly observed in inorganic–organic hybrid structures. Second, the connectivity between the phosphite units and Fe–O–Fe chains give rise to a one-dimensional tancoite-like structure. It has been observed that the one-dimensional iron phosphates, in general, form with the tancoite structure.[27] In **I**, the Fe_2O_{10} dimer replaces the single Fe center in the tancoite structure. The Fe_2O_{10} dimer is, in fact, similar to the Fe_2O_9 and Co_2O_9 dimers observed in the phosphate–oxalate structures.[19,28] The corner sharing between the dimers, observed in **I**, is unique and has been observed for the first time.

The coordination environment of iron centers in phosphates, phosphites, and oxalates presents an interesting

(21) Chitra, R.; Pati, S. K.; Krishnamurthy, H. R.; Sen, D.; Ramasesha, S. *Phys. Rev.* **1995**, *B52*, 6581.
(22) Fisher, M. E. *Am. J. Phys.* **1964**, *32*, 343.
(23) Johnston, D. C.; Kremer, R. K.; Troyer, M.; Wang, X.; Klümper, A.; Bud'ko, S. L.; Panchula, A. F.; Canfield, P. C. *Phys. Rev.* **2000**, *B61*, 9558.
(24) Dzyaloshinskii, I. E. *Sov. Phys. JETP* **1965**, *20*, 665.
(25) Zheludev, A.; Sato, T.; Masuda, T.; Uchinokura, K.; Shirane, G.; Roessli, B. *Phys. Rev. B* **2003**, *68*, 024428.
(26) Choudhury, A.; Natarajan, S.; Rao, C. N. R. *Chem. Commun.* **1999**, 1305.
(27) Cavellec, M.; Riou, D.; Greneche, J.-M.; Ferey, G. *Inorg. Chem.* **1997**, *36*, 2187.
(28) Choudhury, A.; Natarajan, S. *Solid State Sci.* **2000**, *2*, 365.

comparison. The Fe centers in iron phosphates and phosphites, in general, have either five or six coordination forming a trigonal bipyramidal FeO_5 or octahedral FeO_6 building units. In oxalates,[29] oxalatophosphates,[11−16] and also in the present compound, the iron is exclusively present in octahedral environment. It is likely that the average charge per oxygen atom on the oxalate (0.5) is less than to that on the phosphite (0.66) so that more oxalate oxygen atoms are needed to satisfy the valence requirement of iron leading to octahedral coordination.

In conclusion, the synthesis, the structure, and the magnetic properties of a new inorganic−organic hybrid compound of iron, $[C_4N_2H_{12}][Fe^{II}_4(HPO_3)_2(C_2O_4)_3]$, possessing both the phosphite and the oxalate units have been accomplished employing hydrothermal method. Though the structure is formed by the expected building units of FeO_6, HPO_3, and oxalate moieties, the presence of Fe_2O_{10} dimers and the infinite Fe−O−Fe one-dimensional chains are noteworthy structural features. Our continuing investigations reveal that related structures are formed by variations in the initial compositions and synthetic conditions.

(29) Mathoniere, C.; Carling, S. G.; Day, P. *J. Chem. Soc., Dalton Trans*. **1994**, 1551 and the references therein.

Acknowledgment. S.N. thanks the Department of Science and Technology and the Council of Scientific and Industrial Research, Government of India, for the award of a research grant. S.M. thanks the University Grants Commission for the award of a research fellowship.

Supporting Information Available: TGA studies and IR for $[C_4N_2H_{12}][Fe^{II}_4(HPO_3)_2(C_2O_4)_3]$ and M vs H plot at low and high fields. This material is available free of charge via the Internet at http://pubs.acs.org.

CM0501968